CHALMERS
UNIVERSITY OF TECHNOLOGY

Machine Learning Models for Predicting Permanent Deformation in Railway Tracks

Transportation Geotechnics 47 (2024) 101289

Contents lists available at ScienceDirect

Transportation Geotechnics

journal homepage: www.elsevier.com/locate/trgeo

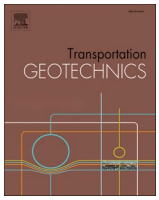

Original Article

Machine Learning Models for Predicting Permanent Deformation in Railway Tracks

Ana Ramos [a,*], António Gomes Correia [b], Kourosh Nasrollahi [c], Jens C.O. Nielsen [c], Rui Calçada [a]

[a] CONSTRUCT-LESE Faculty of Engineering of the University of Porto, Porto, Portugal
[b] ISISE and Department of Civil Engineering of University of Minho, Guimarães, Portugal
[c] Department of Mechanics and Maritime Sciences / CHARMEC, Chalmers University of Technology, Gothenburg, Sweden

ARTICLE INFO

Keywords:
Machine learning algorithms
Permanent deformation in railways
Prediction
Infrastructure
Life-cycle management
Validation

ABSTRACT

To enhance track geometry maintenance planning and reduce infrastructure costs, accurate predictions of accumulated permanent track deformation (settlement) caused by cyclic loading of ballast and subgrade is crucial for railway infrastructure managers. This paper proposes a novel approach to predict long-term settlement with reduced computational cost, based on an extensive parameter study using a hybrid methodology to evaluate both short- and long-term track performance. Various machine learning techniques are compared and employed to develop predictive models, which are validated using measured results from a filed demonstrator of ballasted track. The performance and accuracy of each model are assessed using multiple metrics, and a sensitivity analysis is conducted to identify influential explanatory variables. Notably, the developed random forest model demonstrates good agreement with field measured settlement data. This approach bridges the gap between numerical simulation and empirical data, offering an improved holistic understanding of permanent track deformation. The methodology holds potential for implementation in a computational decision support system for railway track maintenance and renewal management.

Introduction

The long-term settlement of railway tracks, caused by cyclic loading from passing trains, poses significant challenges for railway infrastructure management due to the associated costs and maintenance operations[22]. Consequently, there is a critical need for improved predictive models to better understand the short-term and, more importantly, the long-term performance of the railway systems[25], thereby exploring measures to enhance reliability and reduce life-cycle costs[33].

The subgrade plays a vital role in both short-term and long-term behaviour of the railway tracks, exhibiting two distinct deformations under cyclic loads: resilient and permanent deformations. While resilient deformation influences short-term track performance during a train passages, permanent deformation significantly influences the system's global behaviour over time[17]. Various methods, such as elastoplastic models, shakedown theory, and mechanistic-empirical deformation models, are employed to estimate permanent deformation based on laboratory tests like cyclic triaxial tests. The elastoplastic models are time-consuming as they are dependent on the loading history. Generally, these models only consider a low number of load cycles, which does not agree with *in situ* conditions. The development of these formulations is expressed through conventional concepts such as yield conditions, hardening and flow rules. The main problem with the numerical implementation is that the increment of permanent deformation per cycle soon becomes very small, and this leads to problems with the computational accuracy of the results [1]. The shakedown theory is used to find the shakedown limit of a structure under cyclic load. Indeed, the approach has become very popular in pavement engineering. Here, the main goal consists of preventing excessive permanent strain and guaranteeing that the loading level is below the elastic shakedown limit. However, the assessment is not easy and demands a significant computational effort since it is necessary to consider 3D modelling. The mechanistic-empirical permanent deformation models are simple to use and easy to implement as they describe a relationship between the number of load cycles and accumulated settlement. These models are based on extensive laboratory testing results and depend on fewer

Abbreviations: ML, Machine learning; MRM, Multivariable regression model; DT, Decision tree; RF, Random forest; ANN, Artificial neural network; SVM, Support vector machine; RMSE, Root mean square error; MAE, Mean absolute error; MSE, Mean square error.

* Corresponding author.
E-mail address: aramos@fe.up.pt (A. Ramos).

https://doi.org/10.1016/j.trgeo.2024.101289
Received 3 January 2024; Received in revised form 7 May 2024; Accepted 2 June 2024
Available online 6 June 2024

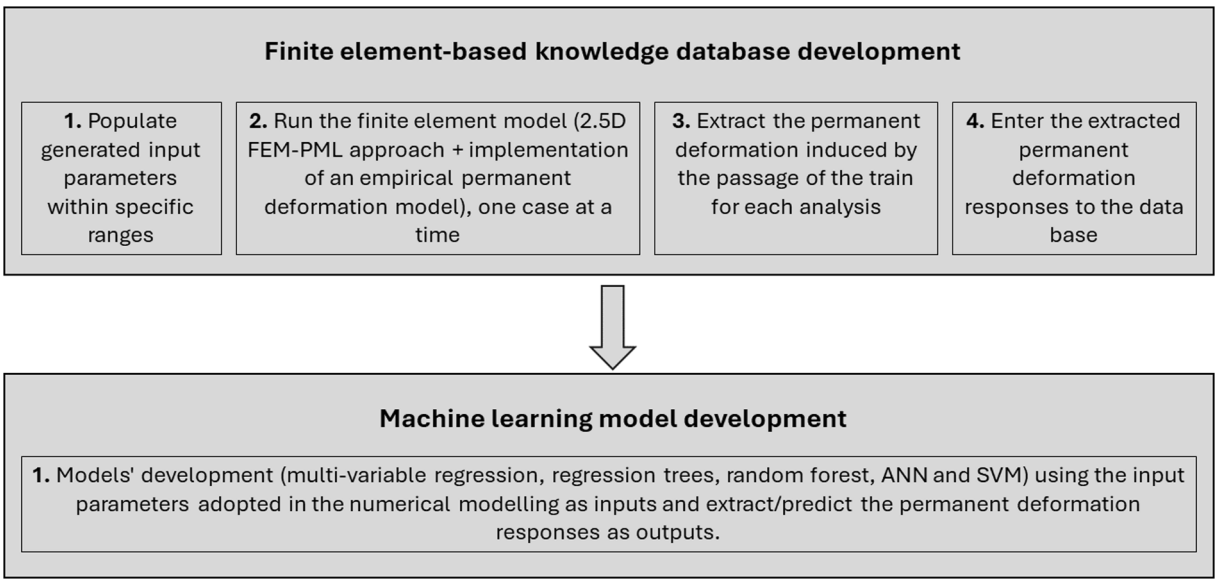

Fig. 1. Overall description of the model development approach.

parameters than conventional elastoplastic models [29].

Addressing this, the paper proposes a novel methodology utilizing machine learning (ML) algorithms to predict permanent deformation and permanent settlement induced in railway systems. While previous studies have focused on prediction short-term performance and resilient modulus, there is a scarcity of works applying ML methodologies for long-term permanent deformation prediction[2,14,15]. ML techniques offer powerful tools capable of establishing complex relationships between predictors and outcomes within a fraction of time, even in geotechnical engineering issues[12,31,36]. Also, several applications of ML algorithms in civil engineering demonstrate their efficiency, including predicting physical and mechanical properties of jet grouting columns, frost depth below pavements, and stiffness properties of airfield pavement, using artificial neural network models[6,8,37,38]. However, few studies have applied ML algorithms for predicting permanent deformation in railway track subgrades within a full model of the vehicle-track system, with most focusing on neural network algorithms[11,13,16,23].

In this paper, in order to determine the best-performing ML models for predicting permanent deformation and respective settlement, five ML algorithms are selected: multivariable regression, decision tree, random forest, ANN and SVM. Each algorithm has its strengths and weakness, and the selection is based on factors like simplicity, accuracy and computational efficiency[19,39]. The methodology proposed accounts for crucial features of the vehicle–track system and is trained on an extensive database of numerical simulation results from a hybrid

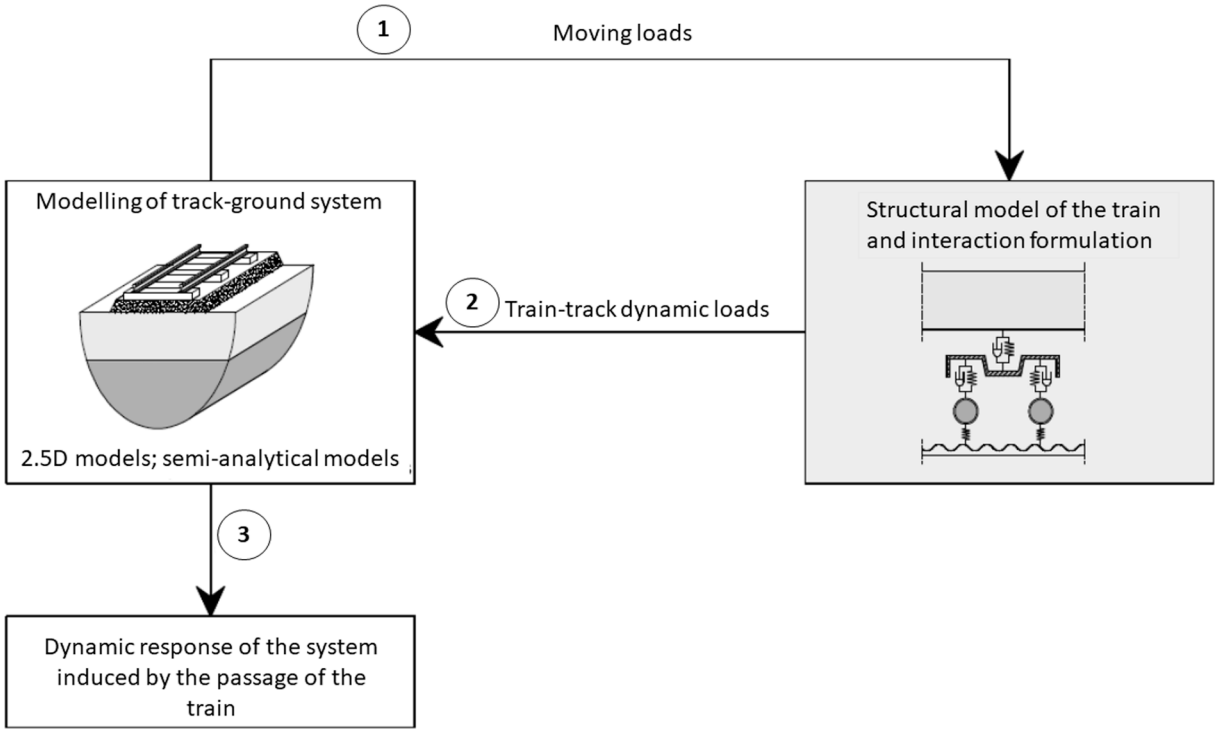

Fig. 2. Flowchart representative of the sub-structured models [26], adapted from [4].

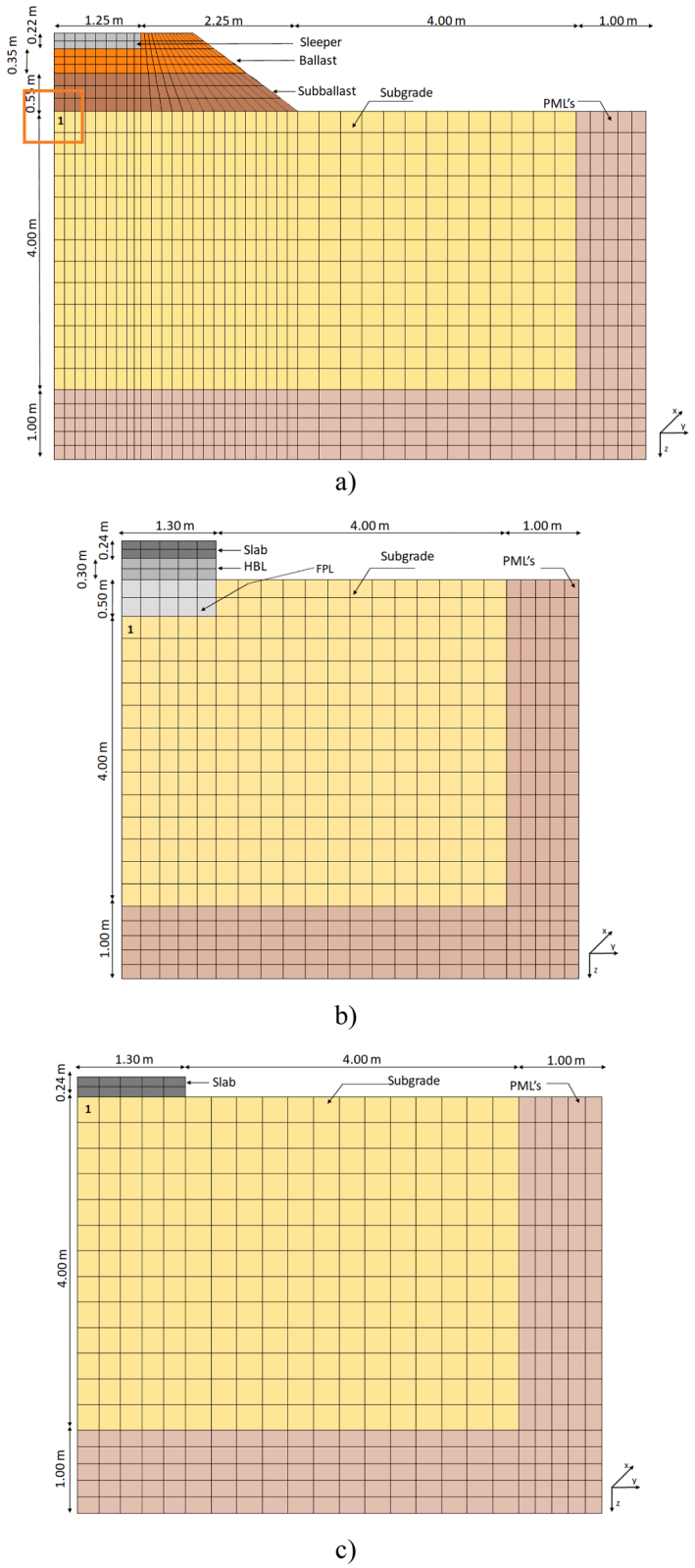

Fig. 3. FEM models of (a) ballasted track, (b) ballastless track (Rheda system), and (c) ballastless track with only a concrete slab [30].

model approach, incorporating a 2.5D FEM-PML track model, including the implementation of an empirical permanent deformation model[26]. The model's performance is enhanced through hyperparameter optimisation.

The inclusion of field experimental validation of ML model distinguishes this research, enabling testing of the model across unseen field conditions. We believe this enhances its effectiveness as a tool for predicting the long-term performance of railway tracks in real-world

Table 1
Summary of variables in the applied database and their range of values (adapted from Ramos et al. [26].

Type of structure	Wavelength interval of unevenness profile [m]	Train speed [km/h]	Mechanical properties of the subgrade (1)			Position along unevenness profile [m]
			M_r [MPa]	ϕ [°]	c [kPa]	
ballasted track	$1 < \lambda < 3$ (2)	80	90	28	0	0
ballastless track	$3 < \lambda < 25$ (3)	144	120	30	5	−85.65
optimised ballastless	$25 < \lambda < 70$ (4)	200	205	35	10	−60.60
track	$1 < \lambda < 70$	300	280	40		−49.6
		360				41.4
		500				

(1) For each combination of resilient modulus and friction angle (90 MPa + 28°; 120 MPa + 30°; 205 MPa + 35°; 280 MPa + 40°), the cohesion was varied (0, 5 and 10 kPa)
(2) The recommended values of the range *D1* were adopted
(3) Designated as *D1* in EN13848-5 [9]
(4) Designated as *D2* in EN13848-5 [9]

scenarios.

FEM-PML model and database

Fig. 1 shows the overall description of the approach for model and database development used in this study. Based on a verified finite element model of a railway track, a knowledge database has been populated. The database contains the generated input parameters (each with a predefined range) and the calculated permanent deformations induced by the passage of a train (based on the number of load cycles). The finite element-based knowledge database has then been employed to train each machine learning model to establish the relationship between the input parameters and the output variable.

Database

This section presents the process used to build the database and the methodology to predict the permanent deformation.

Short-term performance: Model of train–track–ground system

To evaluate the short-term performance of the track, the 2.5D FEM-PML approach has been used. This numerical tool presents a high level of accuracy combined with a reduced computational effort, even when considering the 3D character of the problem[5,34,40]. However, it requires a linear response of the structure and an invariant cross-section along the track. In this case, this is not a problem since the analysis has not considered the existence of any discontinuities/transitions. The assumption of a linear elastic model to represent the soil behaviour is an acceptable simplification of the real constitutive soil behaviour since only small strains are considered.

The simulation of the dynamic interaction of the train–track system is performed using sub-structured models (Fig. 2). The train (modelled by a multi-body formulation, where only the vertical movements are considered) and the track are modelled independently, but compatibility and equilibrium across each interface are imposed. The track–ground system is coupled following a compliance formulation, whereas the compatibility in terms of vertical displacements at each wheel–rail contact is simulated by a linearized *Hertzian* contact stiffness. More details about this methodology can be found in Alves Costa et al. [5] and Alves Costa et al. [4].

To avoid spurious reflections from the boundaries of the track, *Perfectly Matched Layers* (*PMLs*) are added along the boundaries of the domain. These special layers absorb the energy of the waves that impinge the artificial boundaries. This methodology is described in more detail in the work developed by Lopes et al. [18].

Long-term performance: Model of permanent deformation

The cyclic character of the loading induced by passing trains over years of traffic leads to the accumulation of permanent deformation, which, in extreme cases, may even lead to an ultimate collapse of the structure[29].

In this work, an empirical permanent deformation model has been selected to characterise the evolution of the track degradation. The selected model is based on the work by Chen et al. [7] and includes the combined influence of the number of load cycles (N), the initial stress state (p_{ini} and q_{ini}), the stress levels induced in the subgrade during the passage of the train (p_{am} and q_{am}), and also the influence of a *yield criterion* through the inclusion of the parameters s and m directly related to the cohesion and friction angles, respectively:

$$\varepsilon_1^p(N) = \varepsilon_1^{p0}\left[1 - e^{-BN}\right]\left(\frac{\sqrt{{p_{am}}^2 + {q_{am}}^2}}{p_a}\right)^a \bullet \frac{1}{m\left(1 + \frac{p_{ini}}{p_{am}}\right) + \frac{s}{p_{am}} - \frac{(q_{ini}+q_{am})}{p_{am}}} \quad (1)$$

Here parameters ε_1^{p0}, B and a are material constants of the model, p_a is the atmospheric pressure, while m and s are defined by the yielding criterion $q = s + m \bullet p$.

Thus, it is assumed that the long-term permanent deformation is determined based on the short-term response (i.e., stresses generated during the train passage). Then, Eq. (1) is used to calculate the permanent deformation/strain at any given number of load cycles N. The permanent track deformation induced by each axle passage is very small. This means that the simulation process is not carried out cycle by cycle but in increments corresponding to a set of cycles (ΔN). For each set of cycles, it is assumed that the stress state remains constant[28].

Database development

Selection of the variables. To implement a machine learning model for the prediction of permanent deformation, a database has been built based on the parameter study presented in[26]. This parameter study evaluated the influence of several factors on the performance of the subgrade considering three different railway track forms: ballasted track, ballastless track, and an optimised ballastless track only composed of a concrete slab (the support layers were omitted). The numerical model for each type of track form is depicted in Fig. 3. The ballasted track is composed of rails, rail pads, sleepers, ballast, sub-ballast, and subgrade. The ballastless track (*Rheda* system [32] is composed of rails, rail pads, concrete slab, HBL (hydraulically bound layer) and FPL (frost protection layer). The optimised ballastless track is the same as the *Rheda* system except that the HBL and FPL have been omitted.

For a vehicle load model representing a six-car *Alfa Pendular* train, the parameter study was performed by evaluating the stresses of each track form model, see Fig. 3. Only the unsprung mass of each wheelset was considered in the vehicle model. The study included the influence of a track unevenness profile that was artificially generated by superposing 120 wavelengths in a prescribed wavelength interval. The amplitude of

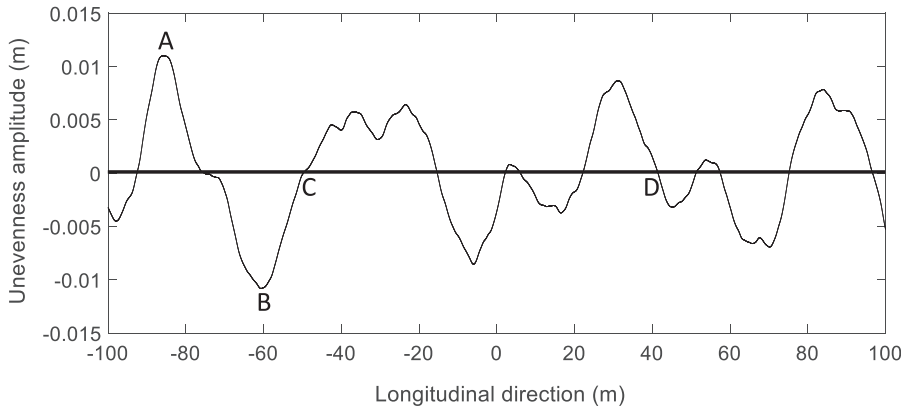

Fig. 4. Selection of considered positions along the unevenness profile.

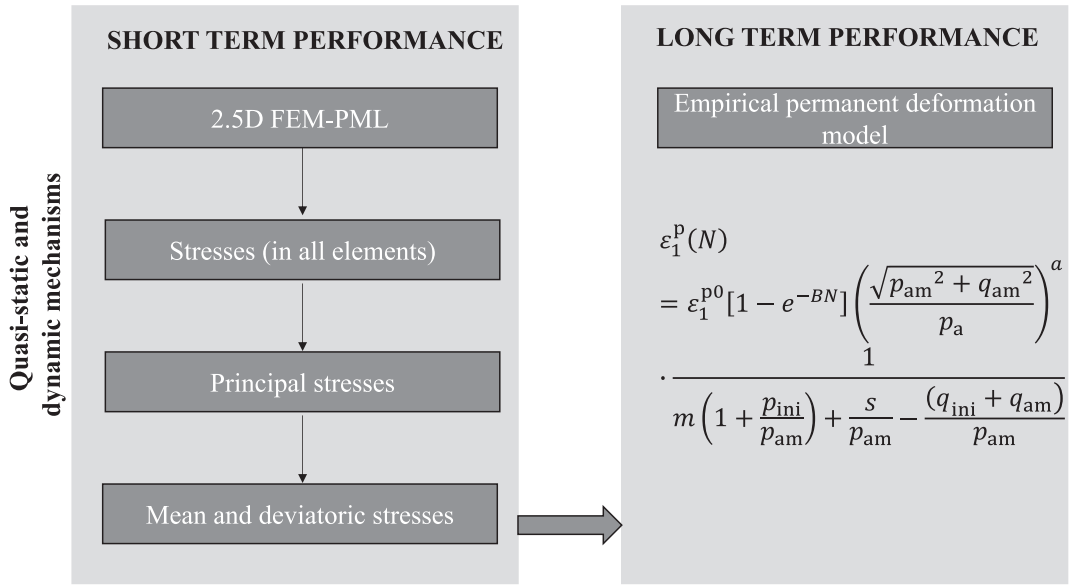

Fig. 5. Flowchart of simulation methodology to build the database.

each wavelength was defined based on the PSD (*power spectral density*) function developed by the FRA (*Federal Railroad Administration*)[3]. More details about the modelling, the obtained results, and the properties of all elements can be found in the work by Ramos et al. [26].

Since different factors had already been analysed in detail in previous work, most of these were considered as input variables to the machine learning models. For these variables, a range of values were adopted. These values were not randomly generated but selected to represent typical conditions in the field. The parameter study included the factors described in Table 1 [26]. Thus, three different railway structures were studied, four different wavelength ranges, four train speeds, different mechanical properties of the subgrade (all possible combinations based on three levels of resilient modulus, four levels of friction angle and three levels of cohesion) and five different positions along the generated unevenness profile (A, B, C, D and the position $x = 0$). The generated unevenness profile is presented in Fig. 4. The five positions were selected to include the positions of maximum and minimum values of the unevenness profile (A and B, respectively), two intermediate positions where there is an increasing or decreasing trend in the unevenness (C and D, respectively), while the position $x = 0$ m was randomly selected. Based on the parameter study [26], it was concluded that the influence of the unevenness profile on the amplification of the dynamic stress and permanent deformation of the subgrade was small. Yet, it was decided to include this variable in this work to evaluate its impact on a machine learning model.

For each combination of variable settings, the maximum, mean and deviatoric stresses (p and q, respectively) were recorded and saved in the database, and they were used as input to the ML models. The number of load cycles (N) and the material constants of the empirical model (ε_1^p, B and a) were also added to the database. This is because empirical and laboratory results (i.e., from triaxial cyclic tests) usually show that the permanent deformation is highly dependent on these parameters[29].

The implemented process is described in Fig. 5. Based on the 2.5D FEM-PML approach and the implementation of the empirical permanent deformation model, the permanent deformation was determined considering the quasi-static and dynamic loading mechanisms. Firstly, the stresses were obtained, as well as the corresponding principal stresses and the mean and deviatoric stresses (short-term analysis). For each given set of input data, the typical simulation time to calculate the short-term response in all elements of the model was about two days since it is necessary to calculate the transfer functions in the frequency domain and then transform the response to the time domain. Posteriorly, these stresses were included in the empirical permanent deformation model. Further, the *yield criterion* and strength parameters, such as cohesion and friction angle, were entered as input/variables, as shown in Table 1. The subsequent simulation of the long-term performance (which also includes the post-processing of the data) was 2–3 h depending on the number of elements and nodes of the track model.

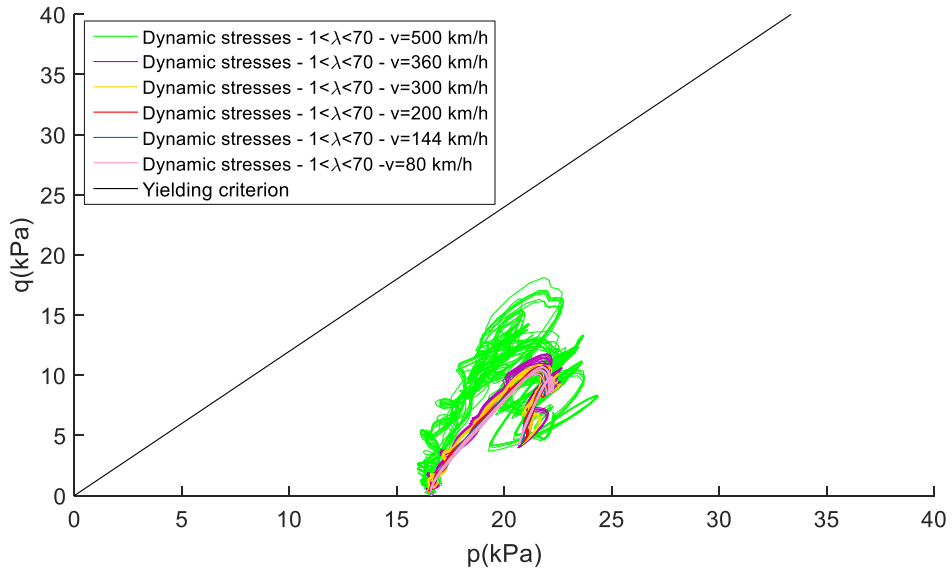

a)

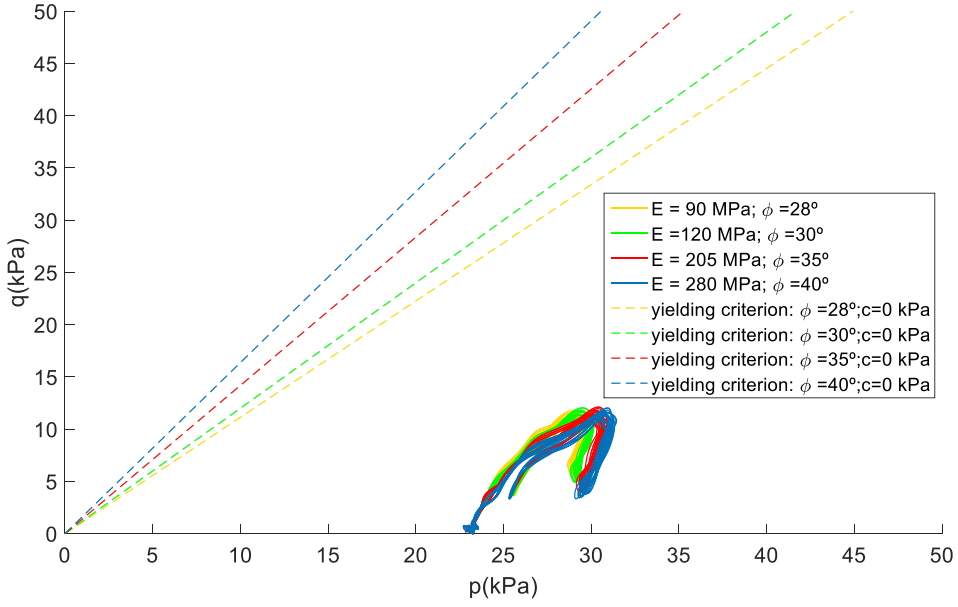

b)

Fig. 6. Examples of calculated p-q stress paths for element 1: (a) influence of train speed on the slab track; (b) influence of the mechanical properties of the subgrade in the ballasted track [26].

Compared to the 2.5D FEM-PML approach described here, the simulation time when using the various machine learning models is negligible.

Each observation in the database corresponds to a single run with the model. Based on the short-term analysis, the values of each variable were recorded and added to the database defined in the software MATLAB. Thus, a database was obtained with the values regarding the type of structure, wavelength, train speed, resilient modulus, position on the unevenness profile and mean and deviatoric stresses, see Table 1. Posteriorly, this shortened database was expanded through the consideration of more variables related to the long-term analysis (number of load cycles, constant of the model, material parameters such as cohesion, friction angle and number of load cycles). Then, the final database was imported into the *R* software [24]. The total number of observations is 186 000. The final database with 186 000 observations is a repetition of the short database but considering the variation of the parameters related with the long-term analysis such as the number of load cycles.

Since the analysis is dependent on the mesh of the model, with this methodology, it is possible to have a more efficient approach and save, for each calculus, 2–3 h per finite element. The main goal is to calculate the permanent deformation of each finite element of the model, as well, as the accumulated permanent settlement (also called cumulative permanent deformation), which is the sum of the permanent settlement of all finite elements along a vertical alignment. Depending on the size of the model, this process may take some time, which can be reduced through the application of the machine learning model.

Examples of calculated stress results (stress paths) are presented in Fig. 6 for the element 1 (identified Fig. 3). This element was selected because of its proximity to the symmetry plane as this simplifies the short-term analysis. These stress paths were calculated in a short-term analysis considering the passage of an Alfa Pendular train. The

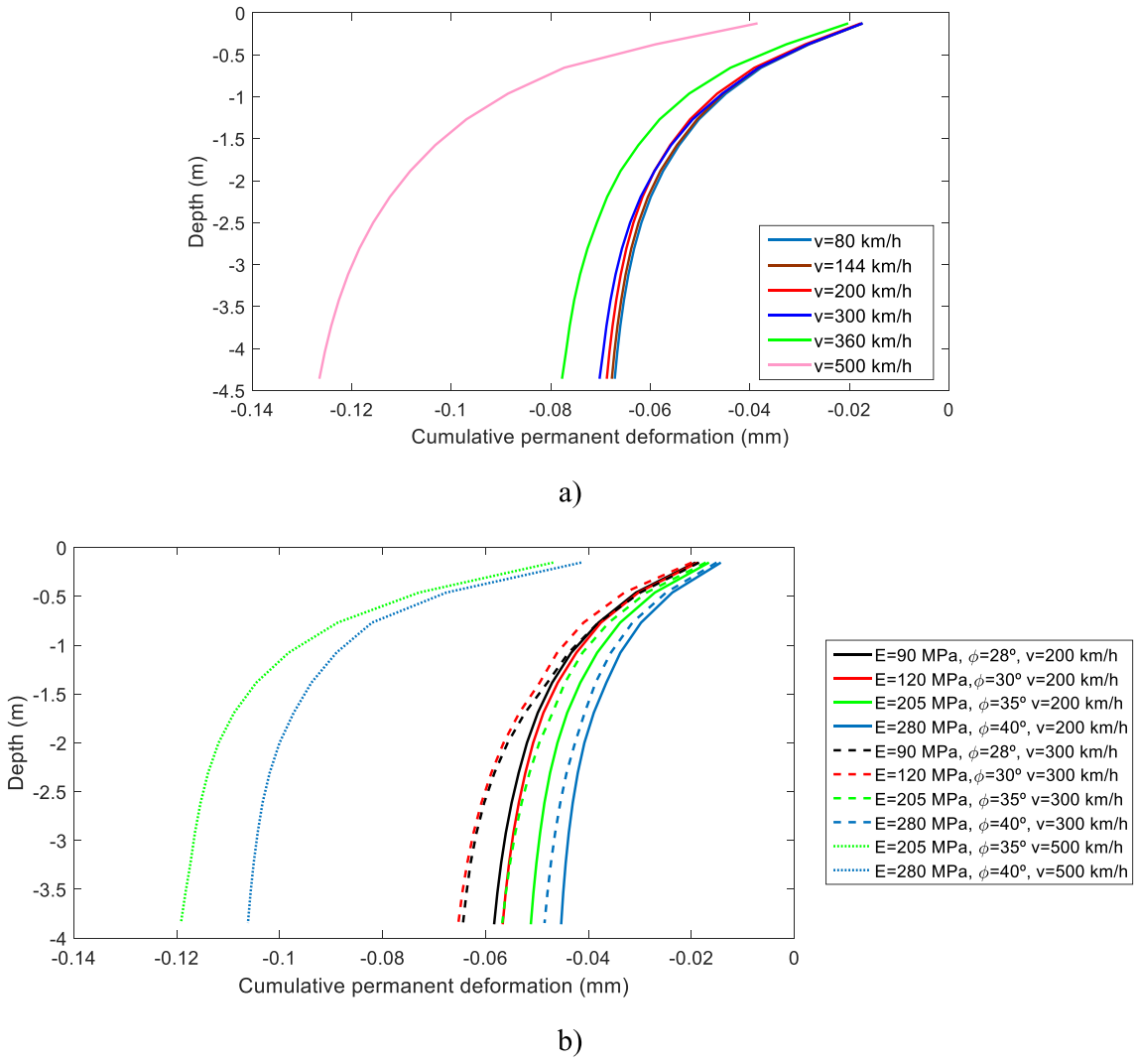

Fig. 7. Examples of cumulative permanent deformation results in the database: a) influence of train speed on the slab track; b) influence of the mechanical properties of the subgrade in the ballasted track [26].

Table 2
Statistical information regarding variables used to predict the induced permanent deformation.

Code	Variable	Abbrev.	Category	Min	Max	Average	Unique values
x1	Ballasted track	B.t	Input	0.000	1.000	0.323	2
x2	Optimised ballastless track	O.bl.T	Input	0.000	1.000	0.323	2
x3	$1 < \lambda < 3$ [m]	$1 < \lambda < 3$	Input	0.000	1.000	0.048	2
x4	$3 < \lambda < 25$ [m]	$3 < \lambda < 25$	Input	0.000	1.000	0.048	2
x5	$25 < \lambda < 70$ [m]	$25 < \lambda < 70$	Input	0.000	1.000	0.048	2
x6	Position [m]	P	Input	−85.650	41.400	−7.473	5
x7	Resilient modulus [MPa]	M_r	Input	90.000	280.000	152.661	4
x8	Cohesion [kPa]	c	Input	0.000	10.000	5.000	3
x9	Friction angle [°]	ϕ	Input	28.000	40.000	31.952	4
x10	Train speed [km/h]	v	Input	80.000	500.000	257.290	6
x11	Maximum deviatoric stress [Pa]	q_{max}	Input	10229.920	26238.190	12914.500	62
x12	Maximum mean stress [Pa]	p_{max}	Input	5660.234	14985.950	7872.714	62
x13	Material constant a	a	Input	0.017	0.650	0.399	4
x14	Material constant B	B	Input	0.006	0.222	0.163	4
x15	Material constant ε_1^{p0}	ε_1^{p0}	Input	0.001	0.429	0.091	4
x16	Number of load cycles	N	Input	1	996,001	498,001	250
Y	Permanent deformation (%)	ε_1^{p}	Output	0.002	2.459	0.295	152,250

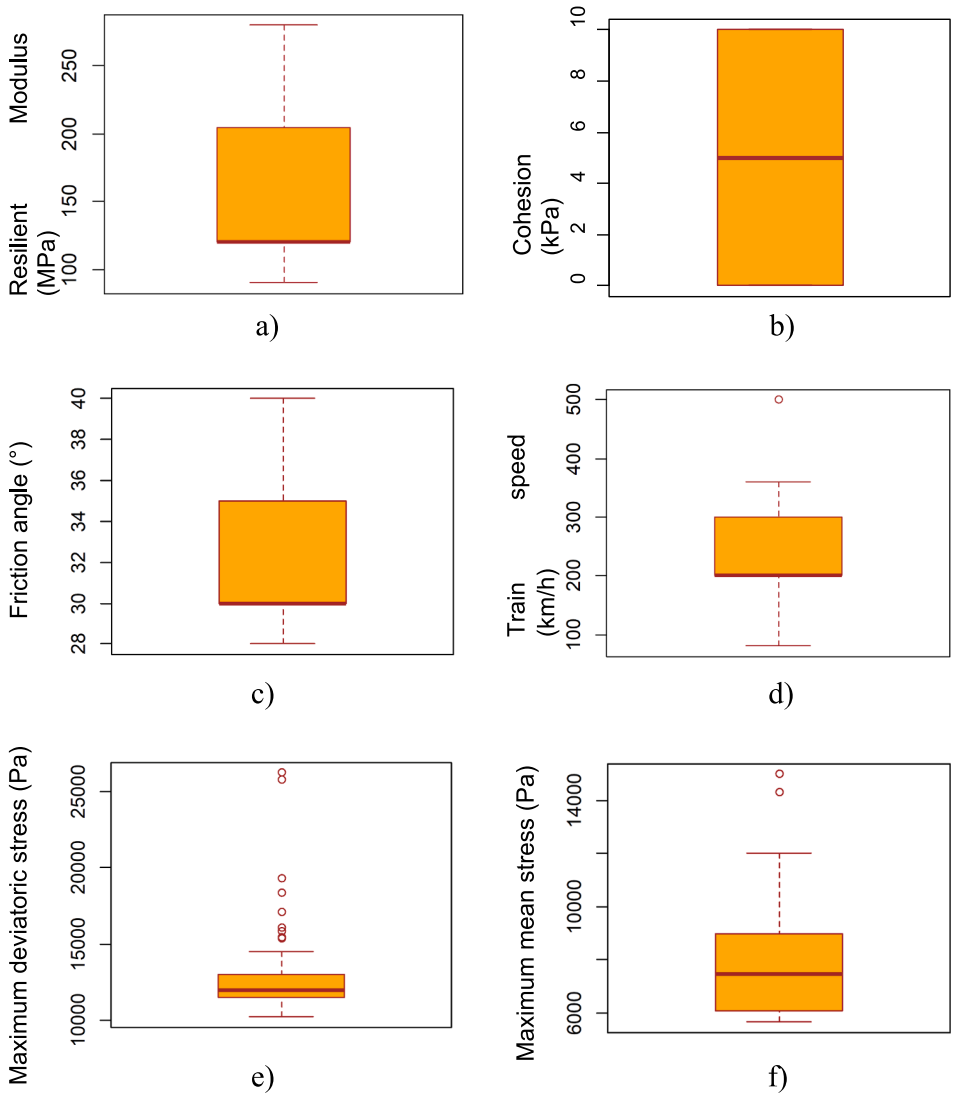

Fig. 8. Box plots of variables: (a) Resilient modulus; (b) Cohesion; (c) Friction angle; (d) Train speed; (e) Maximum deviatoric stress; (f) Maximum mean stress.

maximum mean and deviatoric stresses are important inputs in the database (p_{max}, q_{max}, respectively). In Fig. 6 a), the yielding criterion was defined considering a cohesion of 0 KPa and a friction angle of 30° (associated with a Resilient Modulus of 120 MPa). In Fig. 6 b), the yielding criterion was defined considering a cohesion of 0 kPa. The friction angle's values associated with each yielding criterion are identified in the figure.

The stress results are then used to calculate the permanent deformation (dimensionless) and the corresponding accumulated settlement (cumulative permanent deformation) in millimeters. Examples of calculated cumulative permanent deformation versus depth from the track surface are depicted in Fig. 7. Thus, at each depth, the permanent settlement is accumulated with the permanent settlement measured at this depth and the previous one. The base of the layer is the depth to which the accumulation of deformations is calculated. This type of graph allows to analyse the rate of accumulation of permanent deformation and which areas are contributing the most, which corresponds to the area close to the surface (steepest curve zone).

Statistical analysis. Each dataset in the database is characterised by 16 inputs/predictors and the predicted variable, which is the permanent deformation. Considering the information in Table 1, two variables "type of structure" and "range of wavelength" are classified as categorical. The structure of these variables needs to be recoded into a set of separated binary variables since this is a regression problem. This process is called "dummy coding", where the original variables containing k different levels are transformed into k-1 numerical dummy variables. In the case of the variable "type of structure", which has three different levels, two dummy variables were created containing the values 1 and 0 corresponding to the settings "yes" and "no" for "ballasted track" and "optimized ballastless track", respectively. In this study, the level/magnitude of permanent deformation at the subgrade level was found to be similar for the ballasted track and the ballastless track [26]. The decision not to code the level ballastless track stems from a common practice in data modeling. In order to mitigate bias, it is often advisable to refrain from coding the largest group. This approach aims to prioritize the utilization of the most differentiating variables when constructing the model, thereby minimizing potential biases in the analysis. In this case, the "optimised ballastless track" shows a major influence on permanent deformation because the induced permanent deformation was found to be significantly higher[26]. The same methodology was applied for the "range of wavelength" variable. Here three dummy variables were created: $1 < \lambda < 3$, $3 < \lambda < 25$ and $25 < \lambda < 70$ [m], while the variable $1 < \lambda < 70$ [m] was not coded.

To summarise, each dataset is characterised by the variables presented in Table 2. In the models, these variables are identified by the

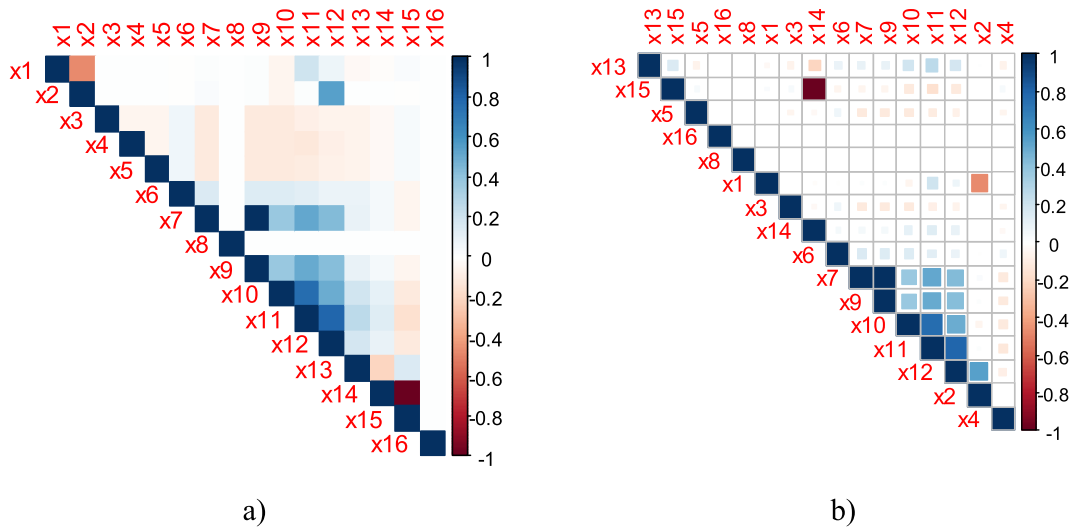

Fig. 9. (a) Correlogram, and (b) correlogram with statistically significant results (*p-value* < 0.01).

following designations x_i ($i = 1, 2, 3, \ldots, 16$). Thus, considering that the problem can be characterised by the expression $y = f(X)$, then X = {*x1, x2, x3, x4, x5, x6, x7, x8, x9, x10, x11, x12, x13, x14, x16*}.

The software *R* was used to perform the prediction of the permanent deformation using the different machine learning algorithms listed in Section 2. Since some variables can be expected to have a higher influence on the permanent deformation, these will be further evaluated in a sensitivity analysis in Section 5. In this case, there are no missing values since the database was repeatedly filled during the process described in Fig. 1 and Fig. 5. The statistical information for each variable that was used for predicting the permanent deformation of the subgrade is provided in Table 2.

Box plots are presented for some selected input variables in Fig. 8. Each of the variables "Resilient modulus," "Cohesion," and "Friction angle" has a regular box plot without outliers, whereas the variable "Train speed" includes one outlier. However, this outlier is important in the prediction of the permanent deformation since this value is very close to the critical speed and leads to an amplification of the permanent deformation. Therefore, this outlier was not excluded from the database. Moreover, the variables "Maximum deviatoric stress" and "Maximum mean stress" also show some outliers. Again, these variables are significant for the determination of the permanent deformation and, thus, the respective observations were kept in the database.

This database can be characterised as multivariate data. The multivariate data allows for defining relationships between two or more attributes. The correlation measure (R^2) is one option, and it presents an advantage in comparison with the covariance since it eliminates the influence of the scale. This correlation presents an indication of the level of linear relationship between two attributes. In this case, a matrix of correlation (correlogram) presents the value of correlation between each pair of attributes. The correlation can be defined by the *Pearson* method (linear correlation), or the *Spearman* method, and the results can be visualized as exemplified in Fig. 9.

The correlogram in Fig. 9 (a) shows very low linear correlations between most variables. Exceptions are the "Resilient modulus" and "Friction angle", which is understandable since there are several empirical expressions that establish a relationship between the Young's modulus of a geomaterial and the friction angle. Indeed, in the parameter study carried out prior to this work, the "Resilient modulus" was defined based on the relationship between this variable and shear wave speed and typical values of N_{SPT} [35]. Moreover, the friction angle was defined based on the expression $\phi' = [15.4(N_1)_{60}]^{0.5} + 20^{\circ}$, which is also dependent on the N_{SPT}.

Furthermore, the variables "ε_1^p", "*B*", "Maximum deviatoric stress", "Maximum mean stress", and "Train speed" show strong correlations. The variables "Ballasted track" and "Optimized ballastless track" also show a high (>0.5) value of correlation. In Fig. 9 (b), only the statistically significant (*p-value* < 0.01) results are presented, which changes the order of the variables in the calculus.

Based on Fig. 9, the variables *x7* and *x9* ("Resilient modulus" and "Friction angle", respectively) show a very high positive correlation (close to 1). This means that one of these variables should be excluded from the permanent deformation model. In this case, the "Friction angle" variable was eliminated.

Modelling process

In the modelling process, the main parameters that influence the quality of each machine learning model have been optimised to improve accuracy. The *k-fold cross-validation* approach has been used to divide the dataset. This methodology allows for the generation of several splits of the training set into training and validation sets to avoid overfitting. The parameter *k* corresponds to the number of different subsets used to split the data. The *k*-1 subsets are used to train the model, while the remaining datasets are used to validate the model. In this case, $k = 10$ was applied. To keep the reliability of the predictions, the same seed was used in the different analyses and tests. Thus, this option assures that the observations in the training and testing datasets are not altered between predictions since this process is performed randomly. In this analysis, five machine learning algorithms were used to predict the permanent deformation.

To evaluate the efficiency, accuracy and robustness of each predictive model, different metrics have been used: R^2, σ, *RMSE*, *MAE* and *MSE*. The R^2 value is the square of the correlation between values that have been predicted and those that have been measured, whereas the standard deviation σ measures how dispersed the data is from the mean. The root mean square error, *RMSE*, represents the standard deviation of the error between the predicted and measured values. The mean absolute error, *MAE*, represents the error that is most likely to occur when the actual values are compared to the predicted ones. The mean square error, *MSE*, measures the average of the squares of the errors, i.e. the average squared difference between the predicted values and the actual value. In this case, the closer the value is to 0, the more accurate is the model.

The R^2, σ, *RMSE*, *MAE* and *MSE* are defined by the following expressions:

Table 3
Machine Learning model 1 - Multivariable regression analysis: coefficients table.

	Estimate	Std. Error	t-value	Pr(>|t|)	Significant. codes
Intercept	9.2E-01	1.1E-02	8.3E + 01	< 2e-16	***
x1	−7.2E-02	2.4E-03	−3.0E + 01	< 2e-16	***
x2	2.1E-01	4.8E-03	4.4E + 01	< 2e-16	***
x3	5.2E-03	3.2E-03	1.7E + 00	0.09773	.
x4	−6.9E-03	3.2E-03	−2.2E + 00	0.03000	*
x5	−1.6E-04	3.2E-03	−5.0E-02	0.96021	x
x6	2.0E-05	2.6E-05	7.7E-01	0.44297	x
x7	−7.3E-04	1.3E-05	−5.5E + 01	< 2e-16	***
x8	−2.9E-02	1.6E-04	−1.8E + 02	< 2e-16	***
x10	3.0E-05	1.1E-05	2.8E + 00	0.00491	**
x11	−5.0E-06	9.5E-07	−5.3E + 00	1.41e-07	***
x12	3.0E-05	1.7E-06	1.8E + 01	< 2e-16	***
x13	−1.1E + 00	2.7E-03	−3.9E + 02	< 2e-16	***
x14	−1.1E + 00	4.9E-02	−2.3E + 01	< 2e-16	***
x15	−1.1E-01	2.3E-02	−4.8E + 00	1.59e-06	***
x16	4.1E-08	2.3E-09	1.8E + 01	< 2e-16	***

Significant. codes: 0 '***' 0.001 '**' 0.01 '*' 0.05 '.' 0.1 'x' 1

$$R^2 = 1 - \frac{RSS}{TSS} \tag{2}$$

$$\sigma = \sqrt{\frac{\sum (x_i - \mu)^2}{N}} \tag{3}$$

$$RMSE = \sqrt{\frac{\sum_{i=1}^{n} (S_i - O_i)^2}{n}} \tag{4}$$

$$MAE = \frac{1}{n} \sum_{i=1}^{n} |S_i - O_i| \tag{5}$$

$$MSE = \frac{1}{n} \sum_{i=1}^{n} (S_i - O_i)^2 \tag{6}$$

where *RRS* is the number of square residuals, *TSS* is the total sum of squares, n is the number of observations, x_i corresponds to each value from the population, μ is the population mean, S_i is the predicted values of a variable, and O_i are the observations.

Multivariable regression model

The first ML model evaluated here is the multivariable regression model. To evaluate the model, the *F-statistic* and the associated *p-value* have been analysed. The result for the multivariable regression model shows that the *p-value* of the *F-statistic* is < 2.2e-16, which indicates a high significance, see Table 3. This means that at least one of the predictor variables is significantly related to the output variable. The coefficients table, see Table 3, shows the estimated regression beta coefficients (column 2) and their associated t-statistic *p-values* (column 5, represented by Pr (>|t|)). These results show that most of the predictor variables are significant, except the variables *x3*, *x5* and *x6*. The predictors with *p-values* less than 0.05 are considered statistically significant, which means there is confidence that the corresponding beta coefficient is not zero. Thus, the beta coefficient does add value to the model by helping to explain the variance within our dependent variable. The standard error (column 3 in Table 3) and t-value (coefficient divided by the standard error – column 4 in Table 3) confirm these conclusions. Indeed, the larger the t-statistic value is, the higher the probability that the beta coefficient is not zero. The t-value is then used to find the *p-value.*

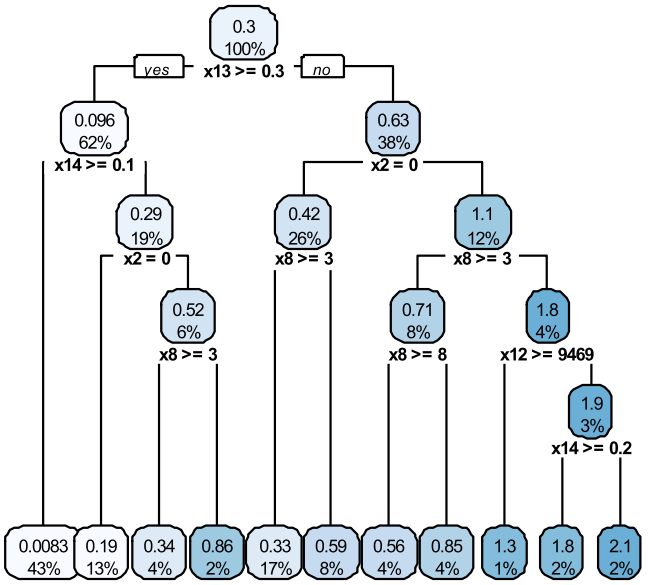

Fig. 10. Machine Learning model 2 - Decision tree.

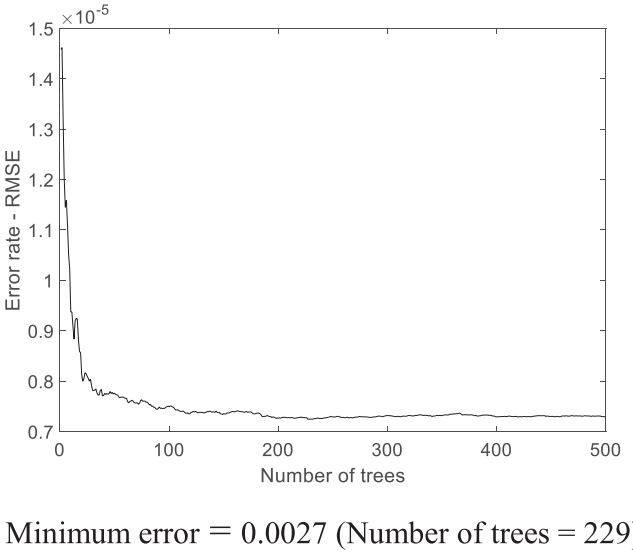

Fig. 11. Machine Learning model 3 - Random Forest: error rate.

In this analysis, the adjusted R^2 is equal to 0.6906, which means that 69.06 % of the variance in the measure of permanent deformation can be predicted with statistical significance by the selected variables. However, one general problem of R^2 is that its value always increases when more variables are added to the model; even if those variables are only weakly associated with the output variable [10]. A solution is to adjust the R^2 by taking into account the number of predictor variables. Furthermore, the result of the multivariable regression analysis shows an *RSE* of 0.227, which corresponds to a 77 % error rate.

Decision tree

Next, the decision tree algorithm was tested. This is a method generally associated with low bias and high variance. This means that it is sensitive to (small) changes in the training data. In this analysis, the

Table 4
Metrics results for the different evaluated machine learning algorithms.

Algorithm	R^2	σ	*RMSE*	*MAE*	*MSE*
Multivariable regression analysis	0.831	0.5271	0.2245	0.1489	0.0504
Decision tree	0.987	0.5690	0.065	0.041	0.0043
Random Forest (best *mtry*)	0.999	0.5715	0.0022	0.0004	4.966e-05
Neural Network	0.999	0.5701	0.0043	0.0027	1.826e-05
SVM	0.998	0.5702	0.0277	0.0235	0.0007

rpart function from the *R* software was used and a pruning value (*cp*) of 0.005 was adopted as it represented the best solution in this case.

The obtained decision tree is presented in Fig. 10. The results show that the variables material constant "*a*" (*x13*), material constant "*B*" (*x14*), "Optimised ballastless track" (*x2*), "Cohesion" (*x8*), and "Maximum mean stress" (*x12*) have the highest influence on the permanent deformation. This information is given by the features used for splitting at the nodes. Features that are used for splitting higher up in the tree or used more frequently can be considered more important and with higher influence on the output.

Random Forest

In order to refine the results, the random forest algorithm was tested. This technique does not require the pre-processing and is very robust to outliers. The main disadvantage is the fact that is less interpretable. Although being accurate, it often cannot compete with advanced boosting algorithms.

In this study, the function *randomForest* from *R* was used. By default, the algorithm performs 500 trees, and the number of variables tried at each split was equal to 3. The performance of the model was evaluated by a plot illustrating the error rate as more trees were introduced. As depicted in Fig. 11, the error rate stabilises with around 100 trees but it continues to converge slowly until around 500 trees (the maximum value adopted). The figure also indicates the minimum error and the associated number of trees.

Furthermore, the number of candidate variables to select at each split set was tested and the function *tuneRF* was used to find the best/optimal value of *mtry* that leads to the smallest error, which means that the best value of *p* is determined.

Artificial neural network

In order to try to improve the results even more, the neural network algorithm was investigated. In these analyses, the model was tested numerous times and the number of hidden layers was tried and optimised. In this case, the number of hidden layers was 2 with 10 and 2 neurones, respectively. Moreover, resilient backpropagation with weight backtracking was adopted. The data was normalized before splitting the database into sets for training and testing. In this analysis, the single output corresponds to the "Permanent deformation" (*y* variable), while 15 input variables were included in the model. Moreover, the package "*neuralnet*" was used to develop the model.

SVM – Support vector regression

Finally, the SVM was adopted using the package *e1071* (from *R)*. This function automatically detects if the model is dealing with a classification or a regression problem. In this case, no hyper-parameterization was tested, which means that the parameters *Cost* and *gamma* were not tuned. This algorithm is different from traditional linear regression methods since it finds a hyperplane that best fits the data points in a continuous space, instead of fitting a line to the data points. Indeed, this algorithm focuses on identifying a hyperplane that maximizes its proximity to numerous data points within a defined margin. This strategy minimizes prediction errors and enables to address non-linear connections between input and target variables through kernel functions.

Results and discussion

As described in Section 3, the performance of each model was analysed in detail based on the R^2, σ, *RMSE*, *MAE, MSE* metrics. The results are presented in Table 4. Based on their performance indices for the training and testing datasets, see Indraratna et al. [16], the models are ranked in Table 5. It is important to note that the results of the permanent deformation are presented in percentage ($\varepsilon_1^p \times 100$).

The multivariable regression analysis model, see Table 4, shows satisfactory results but very far from optimal. Despite the relatively high value of R^2 (>0.6), the *MAE* and *RMSE* are high, which indicates a problem with the model. The metrics for the decision tree model show satisfactory results and an improvement compared to the multivariable regression analysis model (the R^2 increased and the RMSE and MAE and MSE significantly decrease but remains higher taking into account the magnitude of the output value. A significant improvement in accuracy (metrics) is obtained for the random forest algorithm. Here, the *metrics* were determined considering the best *mtry*. In this case, the R^2 is close to 1 and the error rates decrease in comparison with the decision tree.

For the neural network model, the metrics also show very low values regarding the *RMSE*, *MAE* and *MSE*, and a high R^2 value. The metrics are much better than the corresponding values for the decision tree and multivariable linear regression model, showing the high potential of this model. However, the RMSE and the MAE are lower in the random forest model. The results for the SVM model show higher values of the *RMSE* when compared to the neural network model. The results may show a higher dispersion when compared to the neural network model.

Based on the testing results, but also the training results, the models have been ranked according to their metrics *MAE* and *RMSE*. The results presented in Table 5 show that the multivariable linear regression (MLR) model has the worst performance. The best performance was obtained for the random forest model. Moreover, the results show that there are no differences in the ranking based on the testing and training metrics. It is important to highlight that these results should also be compared and validated considering a different database, see Section 6.

The observed and predicted values are compared for the random forest and neural network models in Fig. 12. Despite the low value of *RMSE* for both models, it is observed that the dispersion is similar for the neural network model and random forest model since the points are closer to the line $y = x$.

Table 5
Ranking and predictive performance of the machine learning models.

Model	Performance				Ranking				Total Ranking
	MAE- train	*MAE* - test	*RMSE* - train	*RMSE* - test	*MAE* - train	*MAE* - test	*RMSE* - train	*RMSE* - test	
MLR	0.1482	0.1489	0.2242	0.2245	1	1	1	1	4
Decision tree	0.0394	0.0407	0.0631	0.0657	2	2	2	2	8
Random Forest	0.0003	0.0004	0.0019	0.0022	5	5	5	5	20
ANN	0.0026	0.0027	0.0041	0.0043	4	4	4	4	16
SVM	0.0234	0.0235	0.0270	0.0277	3	3	3	3	12

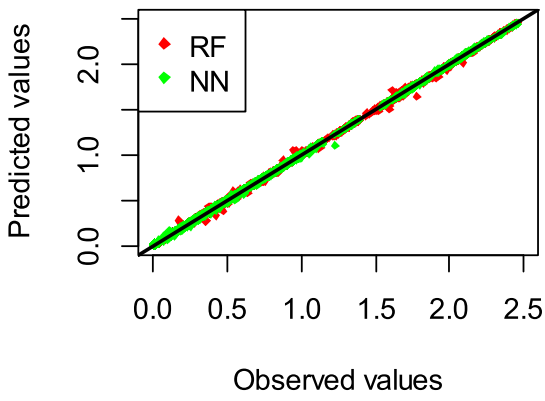

*Scatter plot: predicted values versus observed values of the permanent deformation, in percentage

Fig. 12. Comparisons between neural network and optimized random forest models.

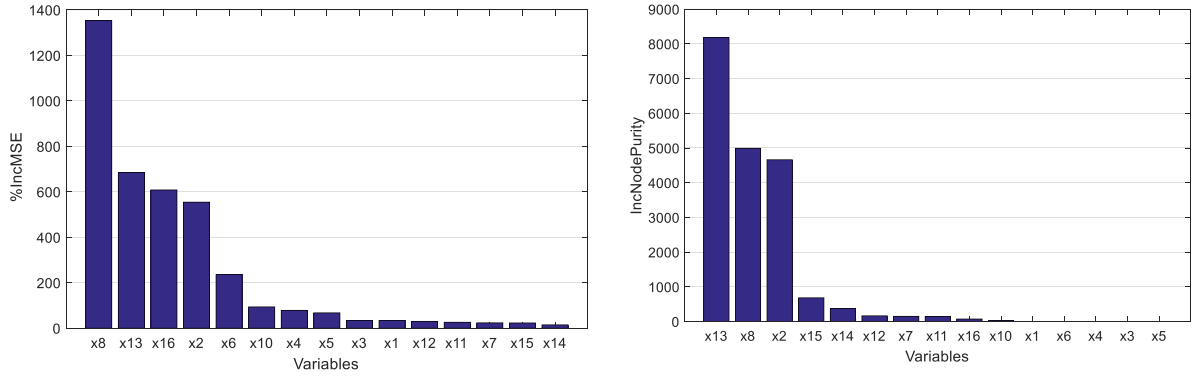

a) Mean decrease accuracy b) Mean decrease Gini

x1	B.t.
x2	O.bl.T
x3	$1<\lambda<3$
x4	$3<\lambda<25$
x5	$25<\lambda<70$
x6	P
x7	M_r
x8	c
x10	v
x11	q_{max}
x12	p_{max}
x13	a
x14	B
x15	ε_1^{p0}
x16	N

Fig. 13. Explanatory variables of machine learning model 3 – Random forest.

Sensitivity analysis

Based on the ranking presented in Table 5, the random forest model showed the best performance. To better understand the model, a sensitivity analysis was performed to determine which variables have the highest influence. The explanatory variables for this algorithm were ranked, see Fig. 13. Here, the mean decrease accuracy shows how much the model accuracy decreases if a given variable is excluded, while the mean decrease *Gini* measures the variable importance based on the *Gini* impurity index used for the calculation of splits in trees.

Despite the significance of variables as indicated in Fig. 13, it is also useful to discuss them based on empirical knowledge about the evolution and development of permanent deformation in the field. The results suggest that the constants ("a", "B", "ε_1^{p0}") of the empirical model, the type of structure/track form, as well as the number of load cycles, have the most significant influence on the permanent deformation. This is in good agreement with observations in the field. Moreover, triaxial cyclic tests show that the mean and deviatoric stresses may influence the development of the permanent deformation. Indeed, by analysing

Table 6
Results with selected (reduced number of) variables in the random forest algorithm.

R^2	σ	*RMSE*	*MAE*	*MSE*
0.999	0.5715	0.0023	0.0004	5.4647e-06

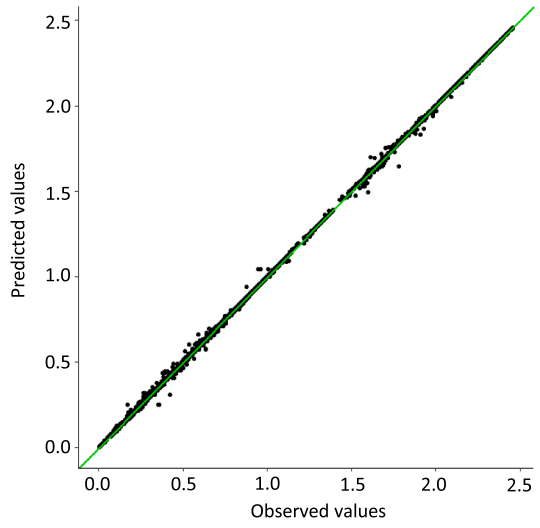

Fig. 14. Scatter plot: predicted values versus observed values (random forest model with reduced number of variables).

Fig. 13 from the random forest model, "Train speed" and "Maximum mean stress" are also identified as explanatory variables besides the previously discussed variables.

To improve the model, an additional analysis was performed where only the explanatory variables with the highest significance were selected: "*x2*", "*x8*", "*x10*", "*x12*", "*x13*", "*x14*", "*x15*" and "*x16*". Again, the random forest algorithm was tested, and the metrics and scatter plot were also determined as well as the importance of each variable.

For the random forest model with a reduced number of selected variables, the corresponding metrics are presented in Table 6. In this case, the metrics remain unchanged when compared to the "original" model. Thus, it is concluded that the random forest model does not need to include the less significant variables to say accurate. This is also confirmed by the scatter plot (Fig. 14), where a very good performance of the model is observed since the predicted and observed values are very close.

In the analysis of the explanatory variables, see Fig. 15, the mean decrease accuracy shows that the reduced random forest model is highly dependent on the "Type of structure – optimised ballastless track" and "Cohesion" of the subgrade, corresponding to variables *x2* and *x8*. The model also shows that the "Maximum mean stress", "Number of load cycles", the constant "*a*" and "*Train speed*" have a significant influence on the developed model. These results demonstrate that the random forest model is very well aligned with empirical knowledge.

Field validation

The preceding sections have established a sense of confidence in some of the developed machine learning models, in particular the random forest and neural network models. In this section, the random forest model will be verified against long-term settlement data measured in the field for the ballasted track at the transition zone[20,21].

Permanent settlements of a track structure have been measured at a test site located on the Swedish heavy haul line in *Malmbanan* at Gransjö, north of Boden. The traffic on *Malmbanan*, a single-track railway line in northern Sweden, is dominated by iron ore freight trains with axle loads up to 32.5 tonnes and speeds of 60 km/h (70 km/h in tare conditions). The annual traffic load is approximately 15 MGT (Mega Gross Tonnes) with around 850 000 axles in loaded and unloaded iron ore trains. Extensive measurements have been carried out in the transition zone between the conventional ballasted track and a 48 m section of a Moulded Modular Multi-Blocks (3 MB) slab track, see Fig. 16(a).

The ballasted track at the test site comprises 60 kg/m rails, rubber rail pads and concrete sleepers. In the slab track section, the rail is

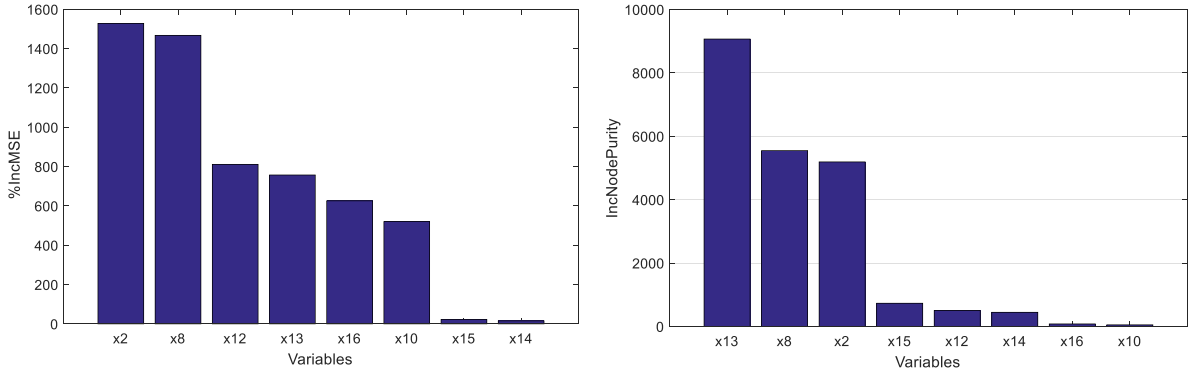

a) Mean decrease accuracy b) Mean decrease Gini

x2	O.bl.T
x8	c
x10	v
x12	p_{max}
x13	a
x14	B
x15	ε_1^{p0}
x16	N

Fig. 15. Explanatory variables of random forest model with selected (reduced number of variables).

Fig. 16. (a) Overview of the transition zone between the ballasted track and 3 MB slab track at Gransjö, Sweden. (b) Detail of an instrumented sleeper equipped with a vertical base plate, an L-shaped mechanism, one accelerometer and one displacement transducer. The positions of the anchor tip and the L-shaped mechanism with a swivel and a roller are shown [20].

Table 7
Adopted properties for the numerical model (adapted from Nasrollahi et al. [20].

Element	E (MPa)	ν	ρ (kg/m3)	α	β
Rail	200×10^3	0.30	7850	–	–
Railpad – ballasted track	97.7	0.45	1200	3.06	7.76×10^{-5}
Railpad – slab track	2.85	0.45	1200	3.06	7.76×10^{-5}
Sleeper	38×10^3	0.15	2500	–	–
Block	30×10^3	0.2	2500	0.61	1.55×10^{-5}
Concrete slab	30×10^3	0.2	2500	0.61	1.55×10^{-5}
Ballast	67.5	0.20	1800	1.84	4.66×10^{-5}
Sub-ballast	161.7	0.30	2100	1.84	4.66×10^{-5}
Soil layer 1	472.4	0.25	2100	1.84	4.66×10^{-5}
Soil layer 2	800	0.25	2100	1.84	4.66×10^{-5}

discretely supported at rail seat distance of 0.6 m. The 3 MB track system is constructed using 4.8 m modules, each featuring a base slab consisting of two longitudinal reinforced concrete beams connected by two transversal beams. In each module, there are also eight precast moulded concrete blocks, with four on each longitudinal beam of the base slab. To reduce the stiffness gradient in the transition zone, under sleeper pads were implemented in the ballasted track. The subgrade at the site consists primarily of moraine extending down to a depth of up to 5 m before reaching bedrock. The embankment height varies between 2.0 and 2.5 m. The properties of ballast, sub-ballast, soil layer 1 and soil layer 2 were defined based on MASW (Multichannel Analysis of Surface Waves) tests performed *in situ*, see Nasrollahi et al. [21]. The properties of the rails, rail pads and sleepers were provided by the manufacturers. A summary of the track properties is presented in Table 7.

A real-time monitoring system was employed to assess the influence of traffic load on the accumulated differential settlement in the transition zone[20,21]. The monitoring took place from September 2022 to June 2023. The vertical sleeper displacements of sleepers 5 and 11 from the transition were measured using fibre Bragg grating (FBG-based) displacement transducers positioned at the end of each sleeper, see Fig. 16 (b). The displacement was measured with respect to a fixed anchor embedded deep in the ground. Both sleepers were initially experiencing a high settlement rate after the installation of the transition zone, see Fig. 17.

To evaluate the performance of this transition zone, a 3D FEM model was developed to mimic the conditions at the Gransjö transition zone,

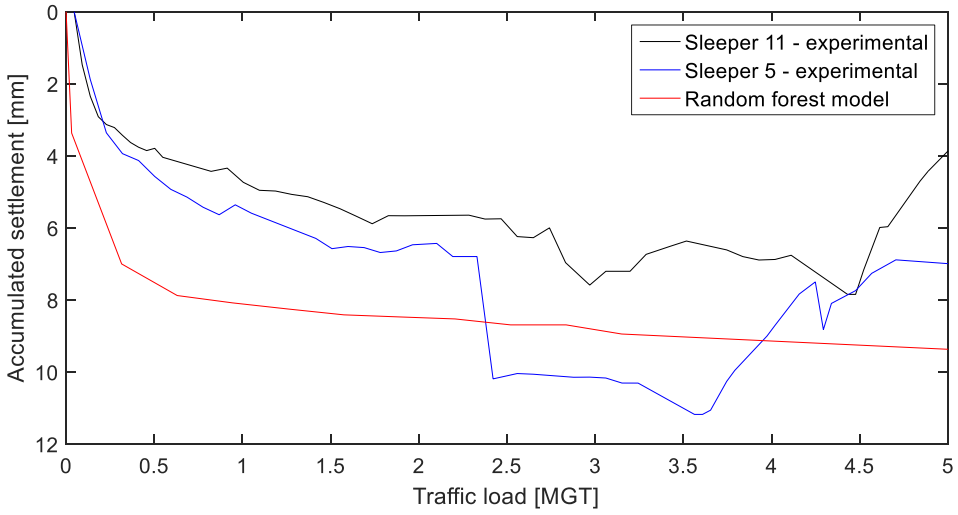

Fig. 17. Measured evolution of unloaded sleeper displacement (settlement) from September 2022 to June 2023 for sleepers 5 and 11 from the transition [20] versus settlement predicted by the random forest model.

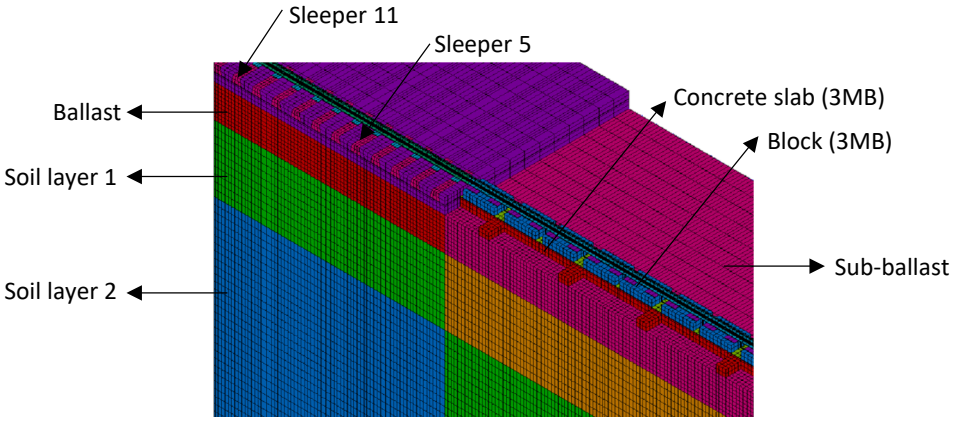

Fig. 18. 3D numerical model of transition zone at Gransjö.

Table 8
Material constants applied in the empirical permanent deformation model.

	Material constant a	Material constant B	Material constant ε_1^{p0}
Ballast	0.65	0.2	0.0093
Sub-ballast	0.65	0.2	−0.000041
Soil layer 1	0.65	0.2	−0.000041
Soil layer 2	0.65	0.2	−0.000041

see Fig. 18. Based on calculated stresses in the short term, the long-term permanent deformation and respective settlement in the transition zone was predicted by the application of the random forest model generated in Section 3. In this analysis, the track type corresponded to a ballasted track and the Resilient Moduli varied according to the material (ballast, sub-ballast, soil layer 1 and soil layer 2), as well as the cohesion. Train speed was set to 60 km/h. For the empirical constants of the model, the values presented in Table 8 were obtained from the work developed by Ramos et al. [26] and Ramos et al. [27].

The mean and deviatoric stresses vary according to the depth of the finite element and the material. The permanent deformation was predicted for each element of the 3D model. Subsequently, the following equation was applied to calculate the cumulative settlement evaluated over the depth of each element of the geomaterials:

$$\delta = \sum_{i=1}^{n} \varepsilon_p^i \times h_i \tag{7}$$

where i represents the number of elements, h_i is the thickness of each element (in m), and ε_p^i is the permanent deformation (dimensionless) of element i obtained through Equation (1).

The predicted long-term deformation of the track and the measured settlements are compared in Fig. 17. It is observed that the random forest model can effectively predict the permanent deformation and permanent (accumulated) settlement in the ballasted track, in particular the trend after about 0.5 MGT. It is important to highlight that the field test data (in particular for sleeper 5) is close to the transition, which usually presents an unpredictable behaviour. This achievement stands as a cross-validation of the random forest model, even within the intricate context of a transition zone.

Conclusions

The prediction of permanent deformation in railway subgrade is crucial for track performance and maintenance cost management. This work introduces a novel methodology utilizing machine learning to estimate permanent deformation. The model is trained on a comprehensive database of numerical simulation results, combining a hybrid 2.5D FEM-PML model and an empirical deformation model. Although the 2.5D model has limitations in accounting for spatially varying parameters of infrastructure along the track, the methodology successfully identifies significant variables affecting track degradation. This encompasses both quasi-static and dynamic mechanisms, with the later incorporating unevenness profile of the track. Various machine learning algorithms (multivariable regression analysis, decision tree, random forest, neural network and support vector regression) are compared by means of different metrics, being random forest yielding the most accurate results, followed by neural networks and support vector regression model. Sensitivity analysis highlights significant variables such as settlement model constants, load cycles, track form, and subgrade strength properties, which are well aligned with what has been observed in the field and previously reported in the specialised bibliography. A simplified random forest model including only 8 variables demonstrates robust performance, indicating its suitability for predictive accuracy of permanent deformation. The random forest model is applied to a Swedish test demonstrator, showing an acceptable predictive capacity of permanent deformation and validating the methodology's effectiveness. The study concludes that this innovative methodology offers efficient and accurate prediction of railway track permanent deformation, with substantial time savings compared to traditional methods.

CRediT authorship contribution statement

Ana Ramos: Writing – original draft, Software, Methodology, Investigation, Conceptualization. **António Gomes Correia:** Writing – review & editing, Supervision. **Kourosh Nasrollahi:** Writing – original draft, Validation, Methodology, Investigation. **Jens C.O. Nielsen:** Writing – review & editing, Validation, Resources, Funding acquisition. **Rui Calçada:** Writing – review & editing, Supervision.

Data availability

The data that support the findings of this study are openly available at https://s.up.pt/tloz.

Declaration of competing interest

The authors declare that they have no known competing financial

interests or personal relationships that could have appeared to influence the work reported in this paper.

Acknowledgments

This work was partially carried out under the framework of In2Track3, a research project of Shift2Rail. This work was also partly financed by FCT / MCTES through national funds (PIDDAC) under the R&D Unit Institute for Sustainability and Innovation in Structural Engineering (ISISE), under reference UIDB / 04029/2020. It has also been financially supported by: Base Funding – UIDB/04708/2020 of the CONSTRUCT – Institute of R&D in Structures and Construction – funded by national funds through the FCT/MCTES (PIDDAC). The field validation chapter (Section 6) is part of the ongoing activities in CHARMEC – Chalmers Railway Mechanics (www.chalmers.se/charmec). Here, parts of the study have been funded from the European Union's Horizon 2020 research and innovation programme in the projects In2Track2 and In2Track3 under grant agreements Nos 826255 and 101012456.

References

[1] Abdelkrim M, Bonnet G, Buhan PD. A computational procedure for predicting the long term residual settlement of a platform induced by repeated traffic loading. Comput Geotech 2003;30:463–76.
[2] Alnedawi A, Al-Ameri R, Nepal KP. Neural network-based model for prediction of permanent deformation of unbound granular materials. J Rock Mech Geotech Eng 2019;11:1231–42.
[3] Alves Costa P. Vibrações do Sistema Via-maciço Induzidas por Tráfego Ferroviário. Modelação Numérica e Validação Experimental. Porto, Portugal: Faculdade de Engenharia da Universidade do Porto; 2011. PhD Thesis.
[4] Alves Costa P, Calçada R, Silva Cardoso A. Track–ground vibrations induced by railway traffic: In-situ measurements and validation of a 2.5D FEM-BEM model. Soil Dyn Earthq Eng 2012;32:111–28.
[5] Alves Costa P, Calçada R, Silva Cardoso A, Bodare A. Influence of soil non-linearity on the dynamic response of high-speed railway tracks. Soil Dyn Earthq Eng 2010; 30:221–35.
[6] Ceylan H, Guclu A, Tutumluer E, Thompson MR. Backcalculation of full-depth asphalt pavement layer moduli considering nonlinear stress-dependent subgrade behavior. Int J Pavement Eng 2005;6:171–82.
[7] Chen R, Chen J, Zhao X, Bian X, Chen Y. Cumulative settlement of track subgrade in high-speed railway under varying water levels. International Journal of Rail Transportation 2014;2:205–20.
[8] Choi H-J, Kim S, Kim Y, Won J. Predicting frost depth of soils in South Korea using machine learning techniques 2022;14:9767.
[9] En13848-5. Railway Applications - Track - Track geometry quality - Part 5: Geometric quality levels. EN13848. Brussels, Belgium: European Committee for Standardization (CEN); 2008.
[10] Gareth J, Witten D, Hastie T, Tibshirani R. An Introduction to Statistical Learning: With Applications in R. Incorporated: Springer Publishing Company; 2014.
[11] Ghorbani B, Arulrajah A, Narsilio G, Horpibulsuk S. Experimental and ANN analysis of temperature effects on the permanent deformation properties of demolition wastes. Transp Geotech 2020;24:100365.
[12] Ghorbani B, Arulrajah A, Narsilio G, Horpibulsuk S, Bo MW. Shakedown analysis of PET blends with demolition waste as pavement base/subbase materials using experimental and neural network methods. Transp Geotech 2021;27:100481.
[13] Ghorbani B, Yaghoubi E, Arulrajah A, Fragomeni S. Long-term performance analysis of demolition waste blends in pavement bases using experimental and machine learning techniques 2023;23:04023058.
[14] Hao S, Pabst T. Experimental investigation and prediction of the permanent deformation of crushed waste rock using an artificial neural network model. Int J Geomech 2022;22.
[15] Hua W, Yu Q, Xiao Y, Li W, Wang M, Chen Y, et al. Development of Artificial-Neural-Network-Based Permanent Deformation Prediction Model of Unbound Granular Materials Subjected to Moving Wheel Loading 2022;15:7303.
[16] Indraratna B, Armaghani DJ, Gomes Correia A, Hunt H, Ngo T. Prediction of resilient modulus of ballast under cyclic loading using machine learning techniques. Transp Geotech 2023;38:100895.
[17] Ling X, Li P, Zhang F, Zhao Y, Li Y, An L. Permanent deformation characteristics of coarse grained subgrade soils under train-induced repeated load. Adv Mater Sci Eng 2017;2017:15.
[18] Lopes P, Alves Costa P, Ferraz M, Calçada R, Silva Cardoso A. Numerical modeling of vibrations induced by railway traffic in tunnels: From the source to the nearby buildings. *Soil Dyn Earthq Eng* Volumes 2014;61–62:269–85.
[19] Myles AJ, Feudale RN, Liu Y, Woody NA, Brown SD. An introduction to decision tree modeling 2004;18:275–85.
[20] Nasrollahi K, Dijkstra J, Nielsen JCO. Towards real-time condition monitoring of a transition zone in a railway structure using fibre Bragg grating sensors. Transp Geotech 2023;44.
[21] Nasrollahi K, Nielsen JC, Aggestam E, Dijkstra J, Ekh M. Prediction of long-term differential track settlement in a transition zone using an iterative approach. Engineering Structures 2023;283:115830.
[22] Nielsen JCO, Li X. Railway track geometry degradation due to differential settlement of ballast/subgrade – Numerical prediction by an iterative procedure. J Sound Vib 2018;412:441–56.
[23] Oskooei PR, Mohammadinia A, Arulrajah A, Horpibulsuk S. Application of artificial neural network models for predicting the resilient modulus of recycled aggregates. Int J Pavement Eng 2020:1–13.
[24] R_Core_Team. R: A language and environment for statistical computing. R Foundation for Statistical Computing; 2021.
[25] Ramos A, Correia AG, Calçada R. Prediction model for permanent deformation of railway subgrade using an artificial neural network (in portuguese). Geotecnia 2023;159.
[26] Ramos A, Gomes Correia A, Calçada R, Alves Costa P. Stress and permanent deformation amplification factors in subgrade induced by dynamic mechanisms in track structures. International Journal of Rail Transportation 2021:1–33.
[27] Ramos A, Gomes Correia A, Calçada R, Alves Costa P, Esen A, Woodward PK, et al. Influence of track foundation on the performance of ballast and concrete slab tracks under cyclic loading: Physical modelling and numerical model calibration. Constr Build Mater 2021;277:122245.
[28] Ramos A, Gomes Correia A, Calçada R, Connolly DP. Ballastless railway track transition zones: An embankment to tunnel analysis. Transp Geotech 2022;33: 100728.
[29] Ramos A, Gomes Correia A, Indraratna B, Ngo T, Calçada R, Costa PA. Mechanistic-empirical permanent deformation models: Laboratory testing, modelling and ranking. Transp Geotech 2020;23:100326.
[30] Ramos, A. L., Correia, A. G., Calçada, R. & Costa, P. A. 2018. Influence of permanent deformations of substructure on ballasted and ballastless tracks performance. Proceedings of 7th Transport Research Arena TRA. April 16–19, 2018 Vienna. Zenodo: Austria; 2018.
[31] Rezaei-Tarahomi A, Kaya O, Ceylan H, Kim S, Gopalakrishnan K, Brill DR. Development of rapid three-dimensional finite-element based rigid airfield pavement foundation response and moduli prediction models. Transp Geotech 2017;13:81–91.
[32] Rheda-System. Rheda 2000. Rail One, Germany: Ballastless Track System; 2011.
[33] Sadri, M., Lu, T., Zoeteman, A. & Steenbergen, M. Railway track design & degradation. *In:* DIMITROVOVÁ, Z., ed. MATEC Web of Conferences, 2018 Lisbon, Portugal.
[34] Sheng X, Jones CJC, Thompson DJ. Prediction of ground vibration from trains using the wavenumber finite and boundary element methods. J Sound Vib 2006; 293:575–86.
[35] Sykora DW. Creation of a data base of seismic shear wave velocities for correlation analysis. Geotech Lab Miscellaneous Paper GL-87-26, US Army Eng 1987.
[36] Tinoco J, Correia A, Cortez P, Toll D. Artificial neural networks for rock and soil cutting slopes stability condition prediction. Proceedings of the 2nd GeoMEast International Congress and Exhibition on Sustainable Civil Infrastructures, Egypt 2018 – The Official International Congress of the Soil-Structure Interaction Group in Egypt (SSIGE). 2019.
[37] Tinoco J, Gomes Correia A, Cortez P. Support vector machines applied to uniaxial compressive strength prediction of jet grouting columns. Comput Geotech 2014;55: 132–40.
[38] Tinoco J, Gomes Correia A, Cortez P. Jet grouting column diameter prediction based on a data-driven approach. Eur J Environ Civ Eng 2018;22:338–58.
[39] Won J, Tutumluer E, Byun Y-H. Predicting permanent strain accumulation of unbound aggregates using machine learning algorithms. Transp Geotech 2023;42: 101060.
[40] Yang Y, Hung H. A 2.5D finite/infinite element approach for modelling visco-elastic body subjected to moving loads. Int J Numer Meth Eng 2001;51:1317–36.